EUROPEAN ORGANIZATION FOR NUCLEAR RESEARCH

L3 Note 2748
June 25, 2002

Search for Colour Reconnection Effects in $e^+e^- \rightarrow W^+W^- \rightarrow$ hadrons through Particle-Flow Studies at $\sqrt{s}$=189-208 GeV

The L3 Collaboration

Abstract

We report on preliminary studies of colour reconnection effects in hadronic decays of W pairs with the L3 detector at center of mass energies between 189 and 208 GeV. The analysis is based on the study of the particle flow between jets associated to the same W boson and between two different W bosons in $qqqq$ events.
The interjet activity shows sensitivity to hadronisation models incorporating colour reconnection schemes. A quantitative comparison between our data and Monte Carlo samples with and without colour reconnection is made.

Submitted to the 31^{st} *International Conference on High Energy Physics*
Amsterdam, Netherlands, 24-31 July 2002.

1 Introduction

In the process $e^+e^- \to W^+W^- \to$ hadrons it has been suggested that interactions may occur between the decay products of the two W bosons [1–4]. As a result the colour flow pattern of these events are modified. Colour rearrangement between two colour singlets are expected from simple QCD principles.

The W bosons produced in e^+e^- annihilation decay at short distances (≈ 0.1 fm). Consequently, the hadronisation of the two quark pairs occurs with a large space-time overlap, since the typical hadronic scale is about 1 fm. Colour reconnection (CR) effects are thought to be suppressed in the hard perturbative phase, but may have larger effects in the non-perturbative stage of the hadronisation process [2]. While hard gluons ($E_g > \Gamma_W$) are emitted incoherently by the two original colour singlets only soft gluons could in principle feel the collective action of both systems and thus participate in cross-talk.

According to the string picture the particles produced in the process $e^+e^- \to W^+W^- \to$ *hadrons* in the absence of colour reconnection come from the fragmentation of two coloured strings which are stretched between the two quarks from the two W bosons. In this case the hadrons can be uniquely assigned to a particular W and there is a direct correspondence between the reconstructed jets and the primary quarks from the W boson decays. Energy momentum is conserved for each of the W systems.

In case of colour reconnection the modifications of this simple string topology picture would modify the colour pattern of the events and result in some depletion and/or enhancement of soft particles in specific phase space regions, especially between the jets.

The analysis presented in this note uses the method suggested in [5] to study the particle flow in $q\bar{q}q\bar{q}$ events to search for these particular effects of particle depletion and enhancement.

The results are based on the full L3 data sample taken from $\sqrt{s}$=189 GeV to 208 GeV, corresponding to an integrated luminosity of 627pb^{-1}. Comparisons with various CR models are made at detector level and the compatibility with the existence of CR effects is investigated in the model frameworks.

The L3 detector is described in detail in Reference 6. All results are preliminary.

2 Data sample and event selection

The selection of $e^+e^- \to W^+W^- \to$ hadrons events used in the particle- and energy flow analysis is based on the energy measured in the electromagnetic and hadronic calorimeters and in the tracking chamber. We measure the total visible energy (E_{vis}) and the energy imbalance parallel ($E_{||}$) and perpendicular ($E_{\perp}$) to the beam direction. The number of clusters, defined as objects obtained from a non-linear combination of energies of charged tracks and calorimetric clusters with a minimum energy of 100 MeV, is denoted by N_{cluster}. The selection criteria are:

- $E_{\mathrm{vis}}/\sqrt{s} > 0.7$; $E_{\perp}/E_{\mathrm{vis}} < 0.2$; $|E_{||}|/E_{\mathrm{vis}} < 0.2$; $N_{\mathrm{cluster}} \geq 40$.

In addition the events should have 4 jets reconstructed with the Durham algorithm with $y_{cut} = 0.01$. To reduce the contamination from hard initial state radiation (ISR) and from semileptonic W decays, we apply cuts to reject events with energetic $\gamma, \mu^{\pm}$ and $e^{\pm}$.

For the study of the particle- and energy flow between jets, the initial quark configuration should be well reconstructed with a nearly perfect quark-jet association. Above 189 GeV, the

W bosons produced in e^+e^- annihilation have a non negligible boost and this property is used to select unambiguous topologies in a sample of 4-jet events.

The criteria correspond to cuts on the four interjet angles. The two largest interjet angles should be between 100° and 140° and not adjacent. The two other interjet angles should be less than 100°. This selection guarantees similar sharing of energy between the four primary partons with the two string evolving back to back. These cuts have been chosen by studying Monte Carlo W^+W^- events at $\sqrt{s}$=189 GeV.

The number of selected events, the number of expected events, the selection efficiency and the percentage of correct pairing are given in Table 1 for each energy point. After applying all the cuts the full sample (from 189 to 208 GeV) contains 666 events with an average efficiency of 12% and a purity of about 85% for $e^+e^- \rightarrow W^+W^- \rightarrow q\,\bar{q}q\,\bar{q}$. The background is composed of $q\bar{q}(\gamma)$ events, and ZZ events in similar amounts. Background events from semileptonic W pair decays is found to be negligible (less than 0.3%). For this study the $q\bar{q}(\gamma)$ process has been modeled with KK2F Monte Carlo program [8]. The probability to have the correct pairing between W bosons and the associated jets is estimated to be 91% on average.

$<\sqrt{s}>$ (GeV)	$\mathcal{L}(pb^{-1})$	N_{events}	N_{MC}	ϵ	correct pair
189	176.4	208	226.0	14.2%	88%
192	29.7	38	37.9	14.3%	90%
196	83.7	104	101.0	13.4%	92%
200	84.3	97	91.9	12.2%	93%
202	35.5	36	37.2	11.3%	93%
205	77.8	75	74.8	10.3%	93%
207	138.9	108	120.8	8.9%	91%
198.2	626.6	666	689.6	12.0%	91%

Table 1: Centre of mass energies, integrated luminosities, number of selected events, number of expected events, selection efficiency and percentage of correct jet pairing for the particle flow analysis.

The whole analysis presented in this paper is done by adding the data taken at the different energies together. To do comparisons, the Monte Carlo samples are first simulated at each center of mass energy and passed through a realistic detector simulation which takes into account all time dependent detector effects and inefficiencies. The Monte Carlo distributions are weighted according to the process cross section and the corresponding luminosity at each energy before being added.

The resulting normalised visible energy and thrust distributions after selection are shown in Figure 1 for the complete data sample together with the Monte Carlo predictions. The distributions of the four interjet angles are shown in Figure 2. The agreement between data and Monte Carlo is satisfactory for all the investigated distributions.

3 Flow distributions

The method to build the particle flow distributions is exactly the same as described in earlier notes [5,7]. We start by defining the plane spanned by the most energetic jet (jet 1) and the jet most likely associated to the same W (jet 2) (Figure 3). For each event we project the direction

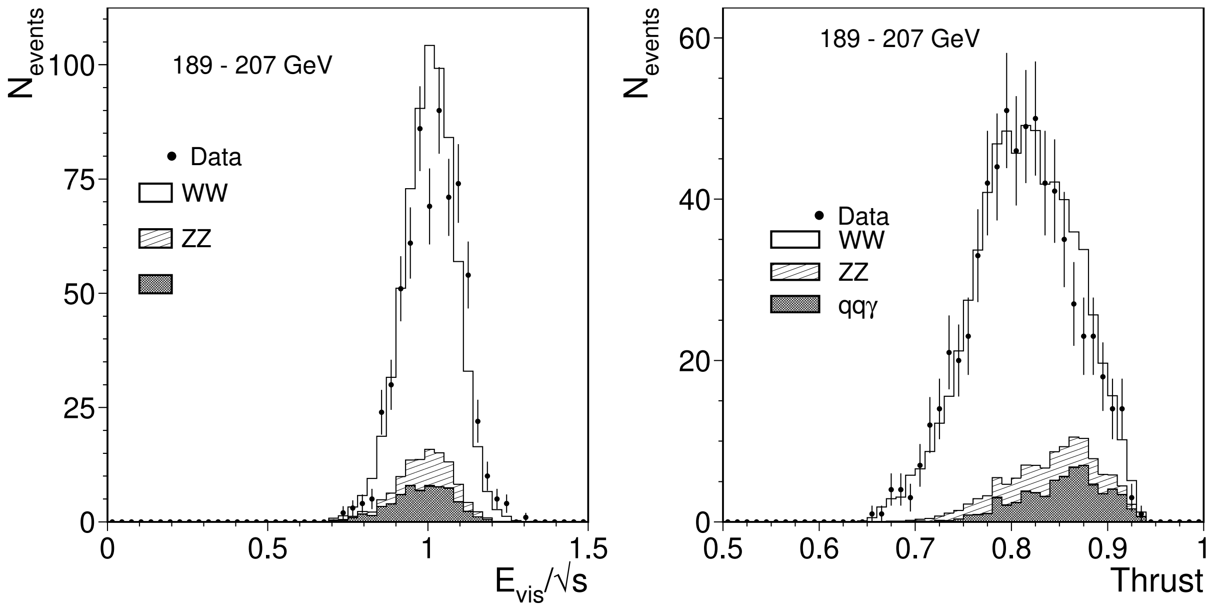

Figure 1: Normalised visible energy and thrust distributions for selected events.

of all the particles onto this plane. The energy and particle flows are measured as a function of the angle on the plane between the jet 1 and the projected momentum vector. This angle is defined as increasing from jet 1 toward jet 2 (from same W), then to the closest jet from the other W (jet 3) toward the remaining jet (jet 4) and back to jet 1. A particle i making an angle ϕ_i with respect to jet 1 adds an entry equal to 1 in the particle flow and adds an entry equal to its energy in the energy flow for the corresponding ϕ bin.

The distributions are calculated using, for the particle definition, the clusters built from tracking and calorimetric information of more than 100 MeV.

The particle flow distribution obtained with those clusters at $189 \leq \sqrt{s} \leq 208$ GeV is shown in Figure 4(left) for the data and the Monte Carlo predictions. Before the background subtraction no normalisation is attempted for particle flow. Figure 4(right) shows the energy flow distribution obtained with the clusters. The contribution of each event to the energy flow is normalised to the total event energy. The data and MC distributions agree over the full angular range.

The 4-jet structure is clearly visible with the decay products of one W covering the region starting from 0 to ≈ 140 degrees while the second W covers the angular region from 140 to 340 degrees.

Having one jet as a reference for all particles makes the direct comparison of the jet1-jet2 particle activity with the jet3-jet4 particle activity difficult. In order to compare the interjet regions the angles on the plane are redefined using a rescaling procedure making use of the relative angle of the particle with the two closest jets. For a particle i located between jets j and k the rescaled angle is: $\phi_i^{\mathrm{resc}} = \phi_i/\phi_{jk}$ where ϕ_{jk} is the angle between jets j and k. With this definition the four jets have fixed rescaled angle values equal to 0, 1, 2 and 3.

A second transformation is performed in order to take into account the fact that the W events are not planar. Figure 5 shows the angle α between the two W decay planes defined by the (jet1-jet2) plane and the (jet3-jet4) plane.

This transformation consists of using four planes for projecting the particles instead of only

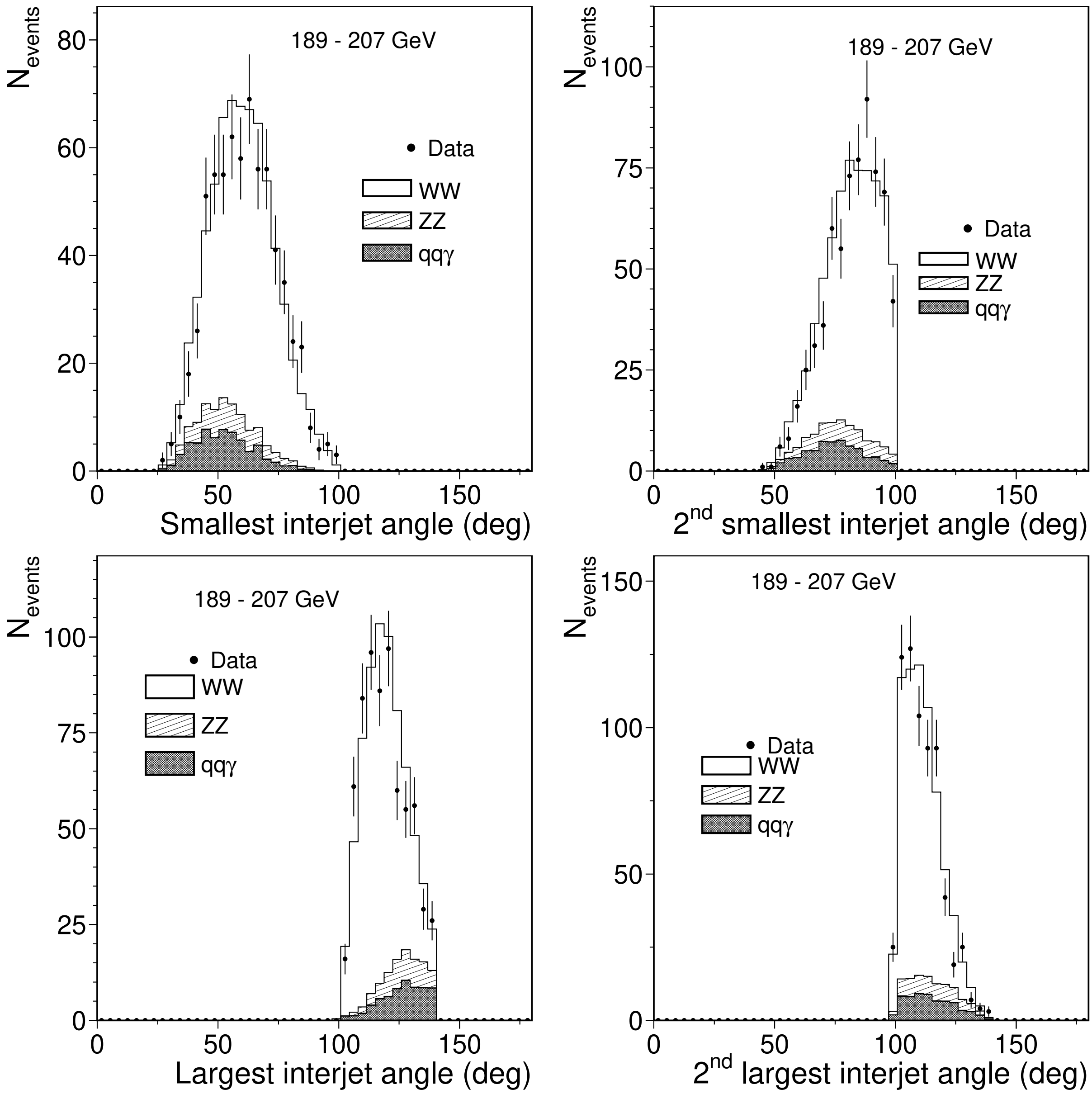

Figure 2: Distributions of the 4 interjet angles after selection.

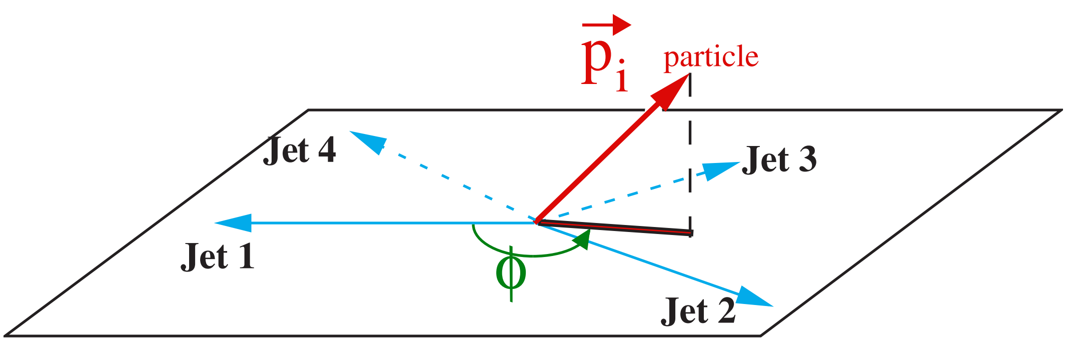

Figure 3: Illustration of the method used to build the flow distributions

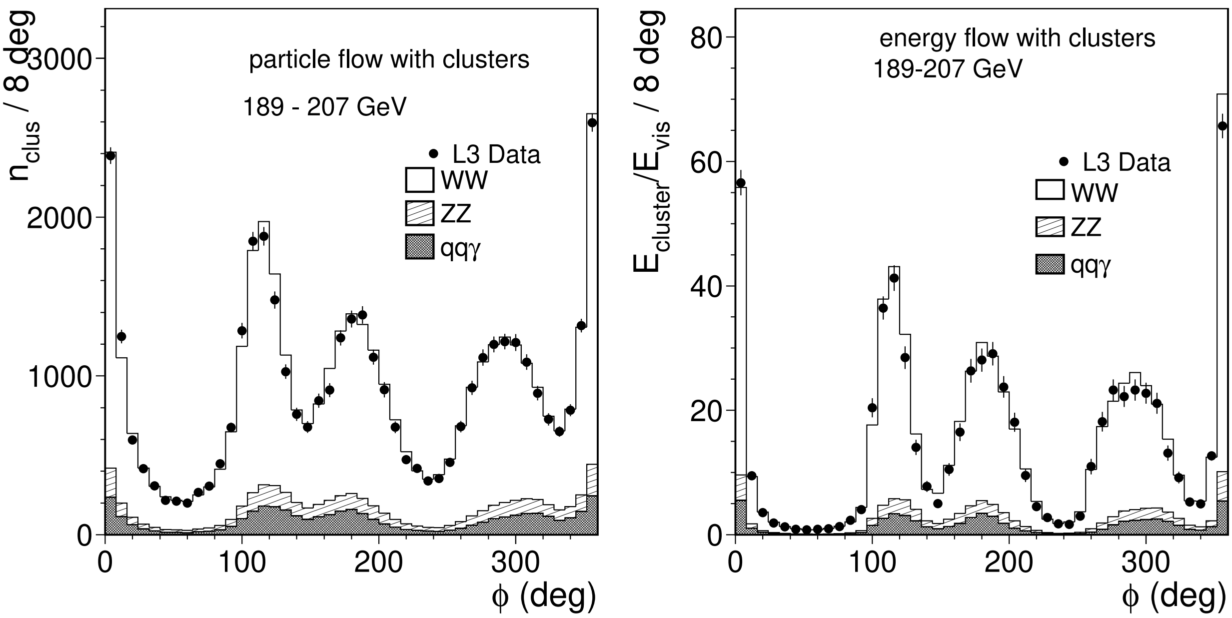

Figure 4: Particle and energy flow distributions obtained with clusters at $\sqrt{s}$ = 189-207 GeV for data and Monte Carlo predictions.

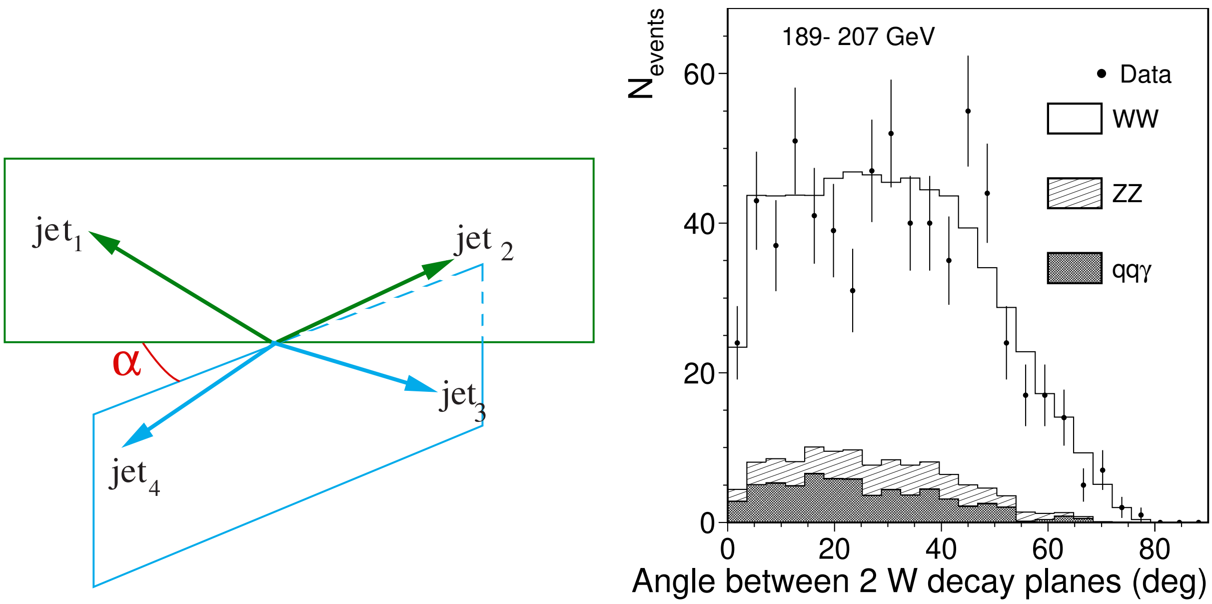

Figure 5: Distribution of the angle between the 2 reconstructed W decay planes at $\sqrt{s}$ = 189 to 207 GeV.

one. The four planes correspond to the planes spanned by each pair of adjacent jets. The particles located between two jets are then projected only on the plane spanned by these two jets. Thus the colour pattern existing between the two partons can be studied.

Figure 6 shows the rescaled normalised particle flow and energy flow distributions after background subtraction for the complete set of data. The line corresponds to the standard KORALW prediction for $q\bar{q}q\bar{q}$ events without colour reconnection. For those events, the LUND string model has been used to describe the parton fragmentation process. It should be noticed that the choice of four planes helps in symmetrising the flow distributions: the interjet activity in the regions corresponding to the two W "strings" in the Monte Carlo are now identical as expected. (This was not the case before this procedure). In the presence of cross-talk between W's such a symmetry may be broken.

3.1 Colour Reconnection Models

The study is performed with CR models which are implemented in the PYTHIA [9], ARIADNE [10] and HERWIG [11] Monte Carlo programs.

The models SKI and SKII [2]implemented in PYTHIA are based on the analogy between coloured strings and superconductors of type I or II with either a finite transverse size or with no lateral extent. The reconnection occurs at the crossing of the two string entities (elongated bags or vortex lines). In the type I model (SKI) the strings are associated to colour flux tubes with a significant transverse extension. The reconnection occurs when these tubes overlap and only one reconnection is allowed, the one with the largest overlap volume. The reconnection probability depends on this volume of overlap and is controlled by one free parameter: k_I which can be varied to generate event samples with different fraction of reconnected events. The relation with the reconnection probability (P_{reco}) is given by the following formula:

$$P_{reco} = (1 - e^{-f.k_I})$$

where f is function of the overlap volume of the two strings which depends on W pair kinematics given by the e^+e^- center-of-mass energy. In this analysis the standard SKI sample is obtained with k_I=0.6 which corresponds to a reconnection propability of about 30% at $\sqrt{s}$=189 GeV. The sample called 100% where all events are reconnected is produced with a k_I value of 10000. An intermediate sample has been produced at all energies with k_I=3.0 corresponding to a reconnection propability of about 66%.

The CR model implemented in ARIADNE is based on reconnection of coloured dipoles before the string fragmentation takes place [12]. In the AR2 scheme, reconnections occur only for emitted gluons with energy less than 2 GeV and a reconnection is allowed only if it reduces the string length.

The CR scheme implemented in HERWIG is, like for the string fragmentation, a local phenomenon since the cluster fragmentation process follows space-time development. In this model [13] the clusters are rearranged if their space-time extension is reduced.

Colour reconnection effects could appear as a depletion or an enhancement of particle production between the quark jets. Figure 7 (top) shows the 189 GeV particle flow distributions obtained with the PYTHIA Monte Carlo at particle level for particles having a momentum greater than 100 MeV. The full line corresponds to no colour reconnection while the dashed line corresponds to the prediction from the SKI 100% model implemented in PYTHIA. The interjet regions corresponding to the two W bosons are named A and B while the interjet regions between two jets from different W's are named C and D as indicated on the plot. We observe

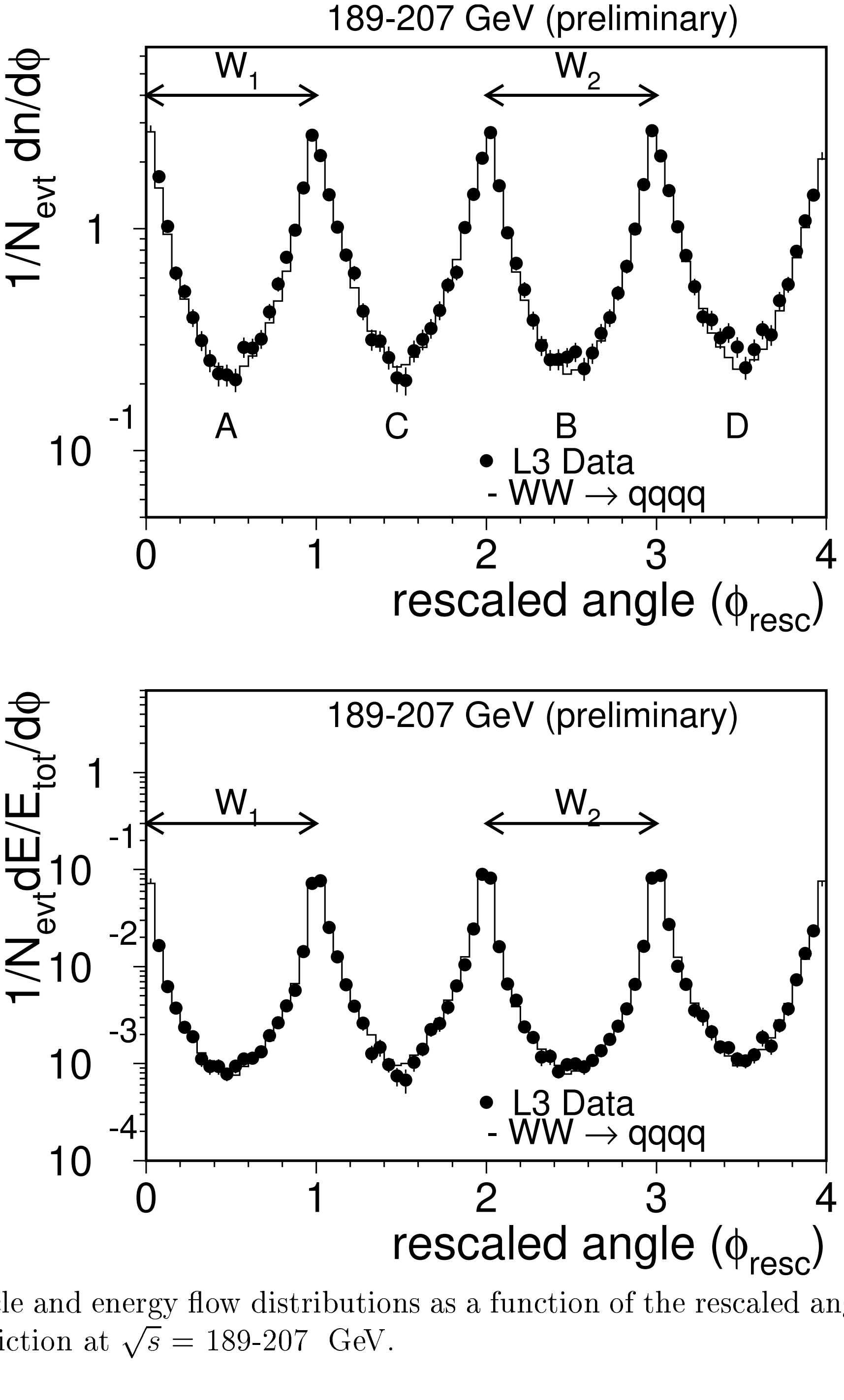

Figure 6: Particle and energy flow distributions as a function of the rescaled angle for data and KORALW prediction at $\sqrt{s}$ = 189-207 GeV.

that the SKI 100% model gives some depletion in the regions A and B and some enhancement of particle rates in the regions C and D, as expected.

For flow distributions computed as a function of the rescaled angle, regions A and B, as well as regions C and D, can be averaged in order to reduce the statistical uncertainty. The averaged results are shown in the two bottom plots of Figure 7. Figure 8 shows the same distributions obtained at detector level using all clusters. The effects seen at the detector level are consistent with the particle level results and have similar amplitudes.

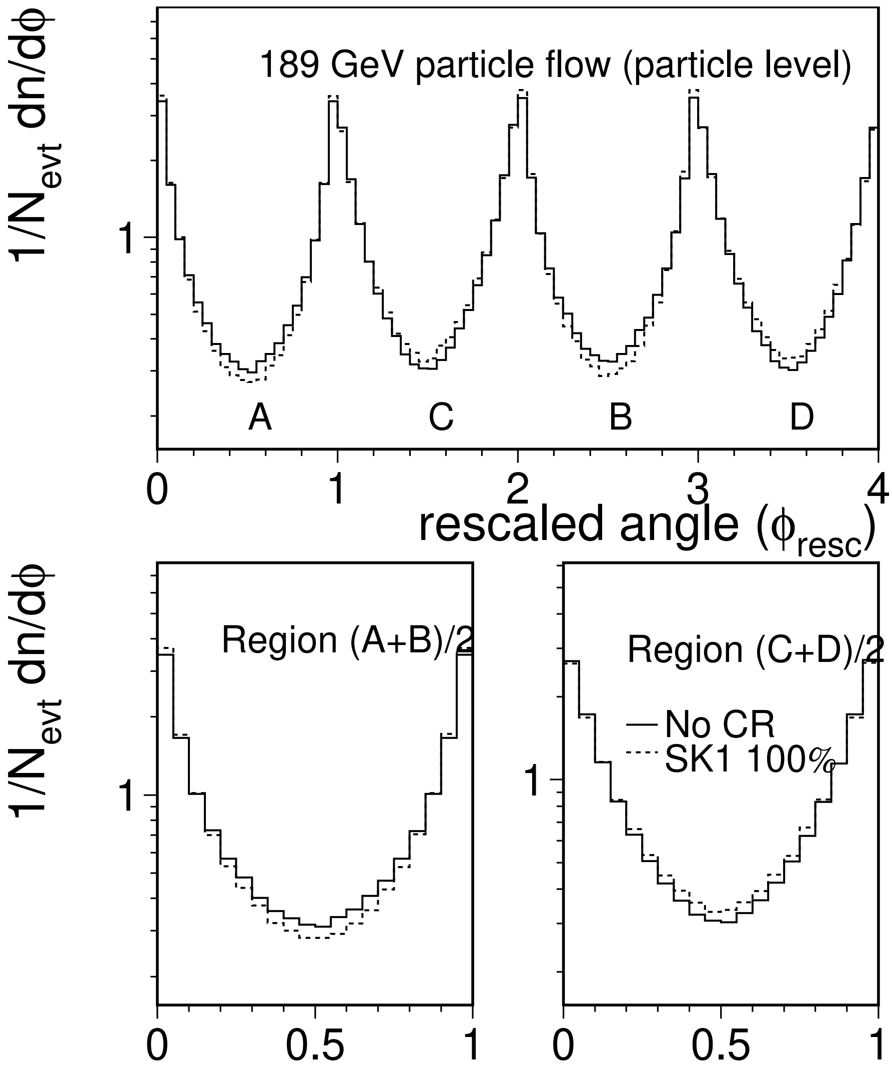

Figure 7: PYTHIA prediction at $\sqrt{s} = 189$ GeV for the particle flow distribution at particle level without colour reconnection (No CR) and for the SKI model with all events reconnected.

3.2 Measured observable

The ratio of the particle activity between the quarks from the same W (regions A+B) and the particle activity between quarks from a different W (regions C+D) is found to be a sensitive observable to the cross-talk effects like the ones predicted by the SKI model. This ratio computed from the energy and particle flow distributions at detector level as a function of the

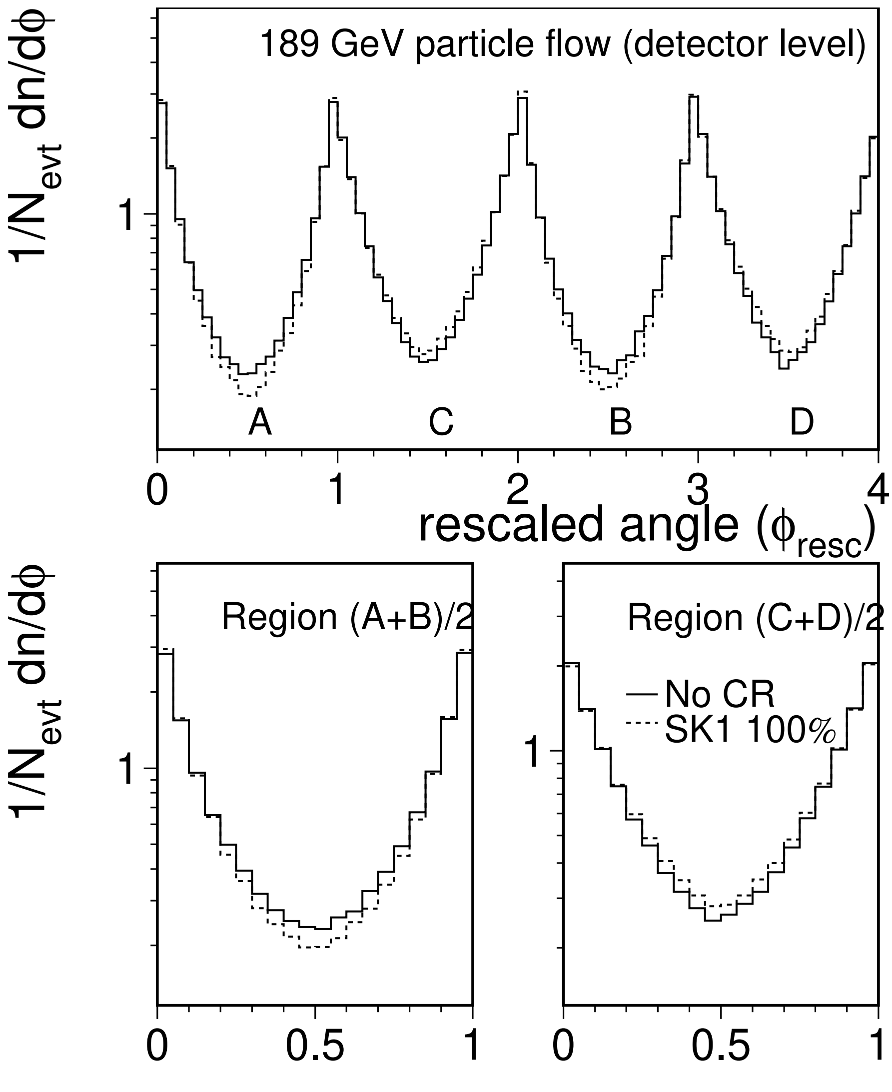

Figure 8: PYTHIA prediction at $\sqrt{s} = 189$ GeV for particle flow distribution at detector level without colour reconnection (No CR) and for the SKI 100% model.

rescaled angle ϕ_{resc} are shown in Figure 9 (left and right) for $\sqrt{s}$=189 GeV to 207 GeV. The full line corresponds to the PYTHIA prediction without CR, the dashed line is the prediction from the SKI (k_I=3.) scenario, and the dotted line corresponds to the prediction of the SKI 100% model. The dots are the L3 data.

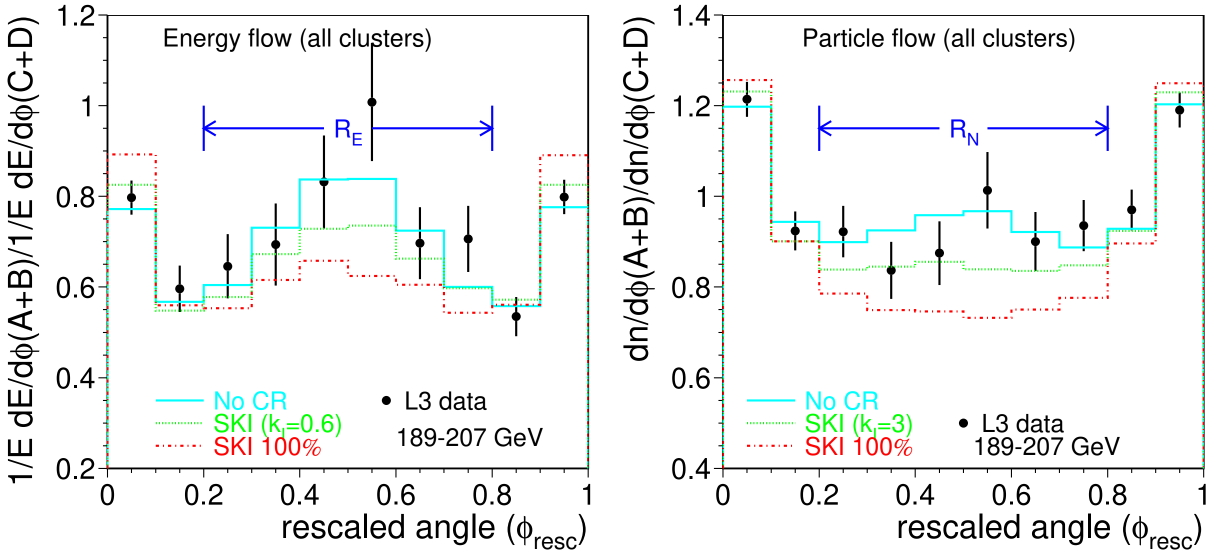

Figure 9: Ratio (R) of the flow distribution in regions (A+B) divided by the flow distribution in regions (C+D) for energy on the left and for particle on the right. The errors shown are statistical.

The differences between the models with and without reconnection schemes are larger in the middle of the interjet regions. Therefore, in order to quantify the colour reconnection effects the ratio R is computed in a restricted ϕ_{resc} interval ranging from 0.2 to 0.8. The corresponding variables for particle and energy flow are defined as follows:

$$R_N = \frac{\int_{0.2}^{0.8} \frac{1}{N_{evt}} \cdot \frac{dn}{d\phi}(regions A{+}B)}{\int_{0.2}^{0.8} \frac{1}{N_{evt}} \cdot \frac{dn}{d\phi}(regions C{+}D)} \quad \text{and} \quad R_E = \frac{\int_{0.2}^{0.8} \frac{1}{E} \cdot \frac{dE}{d\phi}(regions A{+}B)}{\int_{0.2}^{0.8} \frac{1}{E} \cdot \frac{dE}{d\phi}(regions C{+}D)}$$

This interval was originaly [5] proposed to be 0.3 to 0.7. At 189 GeV the two ranges show similar sensitivity to the SKI 100% reconnected event as shown in Table 2. This table shows the MC prediction of the ratio for the No CR sample and the SKI 100% sample together with the expected statistical uncertainty obtained from the data at 189 GeV for various choices of ranges. The sensitivity given in the last column is obtained from the difference between the two MC sample values divided by the statistical uncertainty.

The measured values of R_N and R_E obtained at each center of mass energy are summarised in Table 3. The errors are statistical only. The possible correlations existing in the particle rates between the 4 regions (A, B, C and D) have been taken into account by constructing the full covariance matrix to compute the error. The last row of the table shows the results obtained from the combined data samples. Figure 10 shows the particle flow ratio R_N as a function of the center of mass energy together with MC predictions. The top plot shows a comparison with models without CR effects: KORALW and PYTHIA with and without Bose-Einstein correlations (BEC). The energy dependence originating from the different pairing purities and boost configuration is in agreement with those models. The bottom plot shows the comparison

Range	R_{NoCR}	$R_{100\%}$	ΔR_N(stat)	sensitivity
0.1-0.9	0.889 ± 0.004	0.781 ± 0.004	0.030	3.6σ
0.15-0.85	0.865 ± 0.005	0.735 ± 0.004	0.034	3.8σ
0.2-0.8	0.859 ± 0.005	0.709 ± 0.005	0.037	4.0σ
0.25-0.75	0.863 ± 0.006	0.692 ± 0.005	0.041	4.1 σ
0.3-0.7	0.866 ± 0.007	0.687 ± 0.006	0.047	3.8σ

Table 2: Values of the particle flow ratio computed with the No CR model and with the SKI 100% model at $\sqrt{s}$ =189 GeV for different integration ranges. The sensitivity is defined with respect to the statistical accuracy of the measurement.

with the pythia SKI predictions. The ratio decreases with the reconnection probability over the whole energy range with similar magnitude. The data seems to prefer SKI model with very little colour reconnection.

$<\sqrt{s}>$ (GeV)	R_N	R_E
189	0.820 ± 0.037	0.610 ± 0.047
192	0.929 ± 0.093	0.822 ± 0.133
196	0.948 ± 0.059	0.774 ± 0.077
200	1.004 ± 0.067	0.871 ± 0.095
202	0.770 ± 0.086	0.626 ± 0.130
205	1.033 ± 0.083	0.756 ± 0.111
207	0.958 ± 0.068	0.781 ± 0.096
198.2	0.911 ± 0.023	0.719 ± 0.035

Table 3: Measured R_N and R_E values as a function of energy with their statistical uncertainties.

3.3 Systematic uncertainties

Several sources of systematic errors have been investigated.

- Possible effects coming from Bose-Einstein correlations (BEC) in hadronic W decays have been estimated by repeating the measurements with a Monte Carlo sample with BEC only between particles originating from the same W. The error is obtained by taking half the difference with the default MC which includes full BEC simulation (BE32 option) in W pairs. The sensitivity of the variables to Bose-Einstein correlations are rather small.

- Systematic effect from quark fragmentation modelling in W pair events has been estimated by comparing results using JETSET, HERWIG and ARIADNE Monte Carlo programs. The error is assigned as the spread (R.M.S) between the R_N values obtained with the three fragmentation models.

- Systematic effect from quark fragmentation modelling of the $q\bar{q}$ background has been estimated by comparing results using JETSET and HERWIG Monte Carlo programs. The error is obtained by taking half of the difference between the two models.

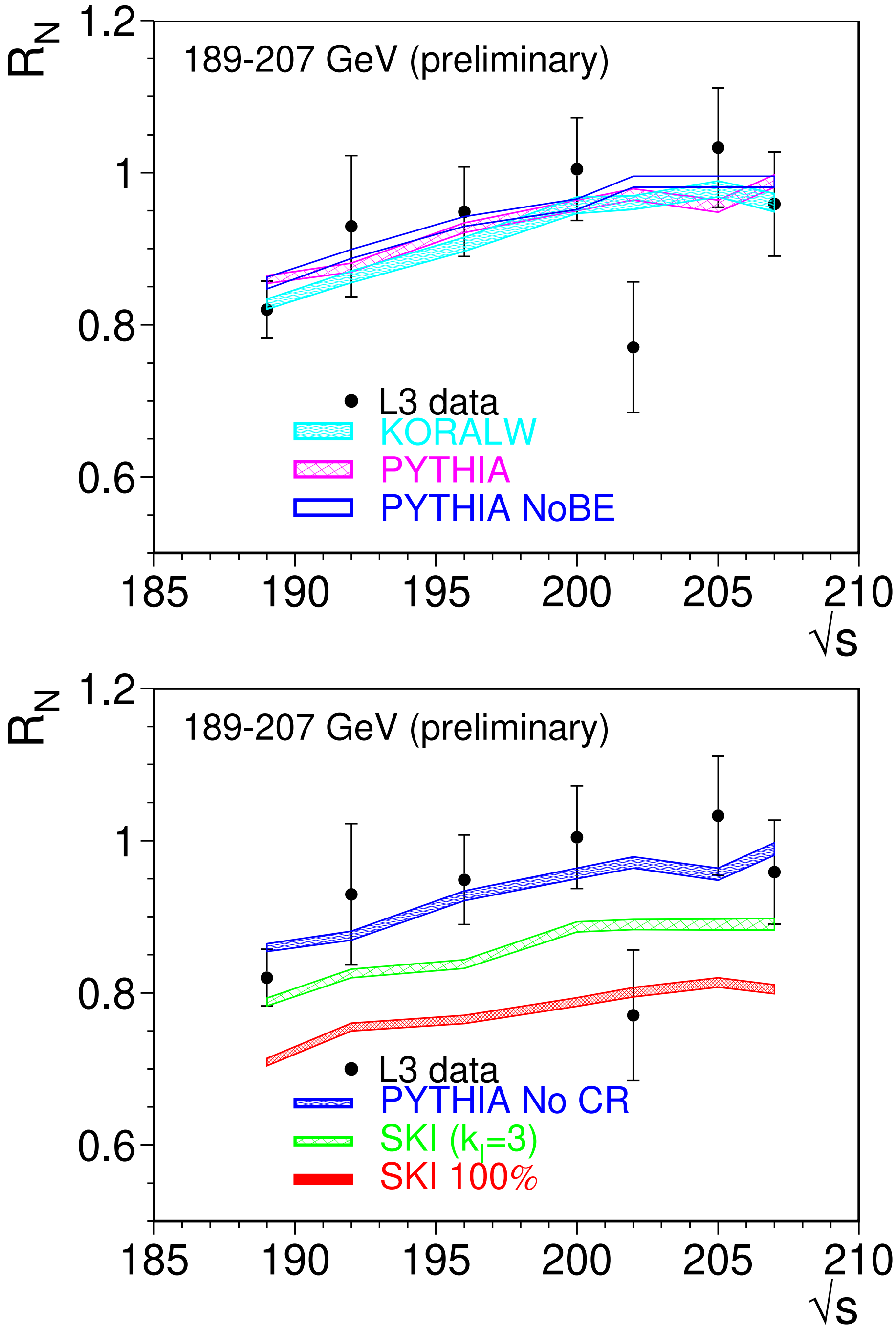

Figure 10: The ratio R_N as a function of $\sqrt{s}$ at detector level for data and several Monte Carlo models without Colour Reconnection (top) and for the PYTHIA SKI model (bottom).

- Since the $q\bar{q}$ background which is subtracted corresponds mainly to QCD 4 jet events which are not well modelled by parton shower program (rate too low) [14] the systematic uncertainty coming from this source has been estimated by varying the corresponding cross-section by ±10%.

- An additional systematic associated to ZZ events is considered. Since these events are subtracted according to the Z pair production cross-section the systematic uncertainty coming from this source has been estimated by varying the corresponding cross-section by ±15%. The resulting error is the smallest contribution to the total systematic uncertainty.

- An other important systematic test is to verify the dependence of the result with the definition of energy flow objects. This is done by comparing results obtained only from calorimetric clusters and results obtained by objects built from combination of track and calorimetric clusters. The latter being the nominal choice. The uncertainty is estimated by taking half of the difference between the two analyses.

A summary of the different contributions to the systematic errors is given in Table 4.

source	R_E	R_N
BEC	± 0.006	± 0.003
Fragmentation	± 0.004	± 0.008
back. fragmentation	± 0.008	± 0.009
$q\bar{q}$ X-sect.	± 0.008	± 0.007
ZZ X-sect.	± 0.003	± 0.002
Flow objects	± 0.017	± 0.016
Total	± 0.022	± 0.021

Table 4: Contributions to the systematic uncertainties on R_E and R_N.

The ratio values obtained with the complete data set are then:

$$\begin{aligned} R_N &= 0.911 \pm 0.023(stat.) \pm 0.021(syst.) \\ R_E &= 0.719 \pm 0.035(stat.) \pm 0.022(syst.)\,, \end{aligned}$$

3.4 Semileptonic W pair decay analysis

The quality of the MC simulation of the $q\bar{q}$ fragmentation process and the possible biases which may arise when determining the particle yields between reconstructed jets in the detector have been investigated by analysing the particle and energy flow in semileptonic WW events. For this analysis the events are selected using criteria based on hadronic events with a large missing momentum and the presence of a high energy electron or muon (p≥ 30 GeV). The missing momentum is considered as an additional particle in order to apply the Durham jet algorithm to select 4-jet events with a y_{cut}=0.01.
The same angular criteria on the four interjet angles applied in the 4-quark case are used for this selection. The purity obtained after selection is about 96% and the efficiency to select $qq\mu\nu$ or $qqe\nu$ events is about 12%. The number of selected semileptonic events for $189 \leq \sqrt{s} \leq 207$ GeV is 315 with an expectation of 314.5 events. Particle flow and energy flow distributions

are built in a similar way as for the 4 quark events with the exception that the charged lepton should be in the jet 3 or 4. Figure 11 (left) shows the corresponding particle flow distribution for $\sqrt{s}$=189 up to 207 GeV. The dots are the data and the line gives the KORALW MC prediction. There is good agreement between data and MC over the whole distribution. The lepton and the neutrino jets give small multiplicity contributions. The plot on the right shows the rescaled particle flow distribution where the different structure of the two different W is clearly visible. The interjet activity in the W_2 region (equivalent to region B in the 4-quark events) is mainly due to low energy fragments from the hadronic decay of the first W. The complete W interjet activity in a 4-quark event without CR effects should be equivalent to summing the regions W_1+W_2 (also called region A+B) of the semileptonic distribution. This point was verified by using MC samples without CR. A comparison between data and MC for

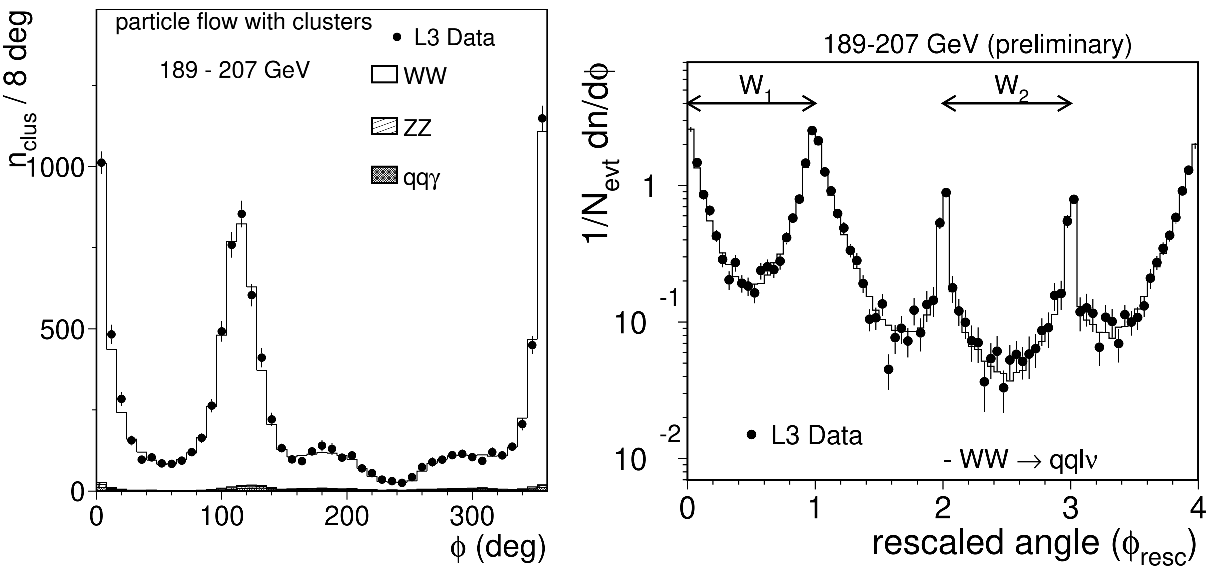

Figure 11: Particle flow distributions at raw level and as a function of the rescaled angle for the semileptonic W decays for data and KORALW prediction at $\sqrt{s}$ = 189-207 GeV.

the particle flow obtained by summing the regions A and B in the semileptonic event is shown in figure 12 (top). The ratio Data/MC of this distribution is shown as a function of the rescaled angle in the bottom part of figure 12. This ratio is consistent with unity over the whole range. This result gives confidence about the modelling of the fragmentation process of a quark pair with the fragmentation parameters used in KORALW or PYTHIA and also about the particle flow definition and reconstruction. To quantify this comparison we construct the following two ratios which use the same angular range as for the 4-quark analysis:

$$R_N^{qql\nu} = \frac{\int_{0.2}^{0.8} \frac{1}{N_{evt}} \cdot \frac{dn}{d\phi}(A+B)Data}{\int_{0.2}^{0.8} \frac{1}{N_{evt}} \cdot \frac{dn}{d\phi}(A+B)MC} \quad \text{and} \quad R_E^{qql\nu} = \frac{\int_{0.2}^{0.8} \frac{1}{E} \cdot \frac{dE}{d\phi}(A+B)Data}{\int_{0.2}^{0.8} \frac{1}{E} \cdot \frac{dE}{d\phi}(A+B)MC}$$

Figure 13 shows the values of these ratios for all the center of mass energies and for the complete L3 data set. The dotted line gives the expected result in the absence of any problem. All the measurements agree with unity within the statistical error and no bias is measured.
This study validates the method and the choice of energy flow objects used to measure the particle yields in the $q\bar{q}q\bar{q}$ events for the colour reconnection analysis.

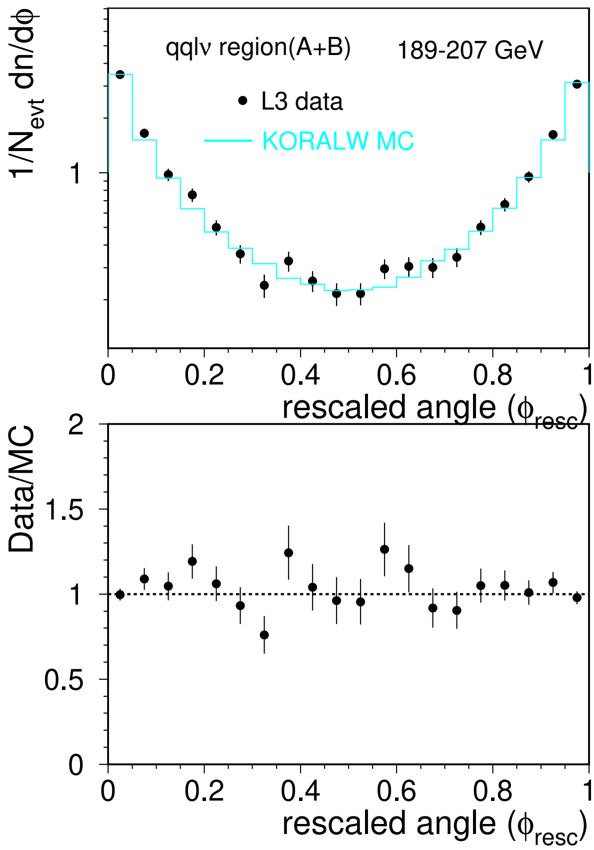

Figure 12: a) Particle flow distributions as a function of the rescaled angle for the semileptonic W decays for data and KORALW prediction at $\sqrt{s} = 189\text{-}207$ GeV. b)Distributio of Data/MC ratio as a function of the rescaled angle

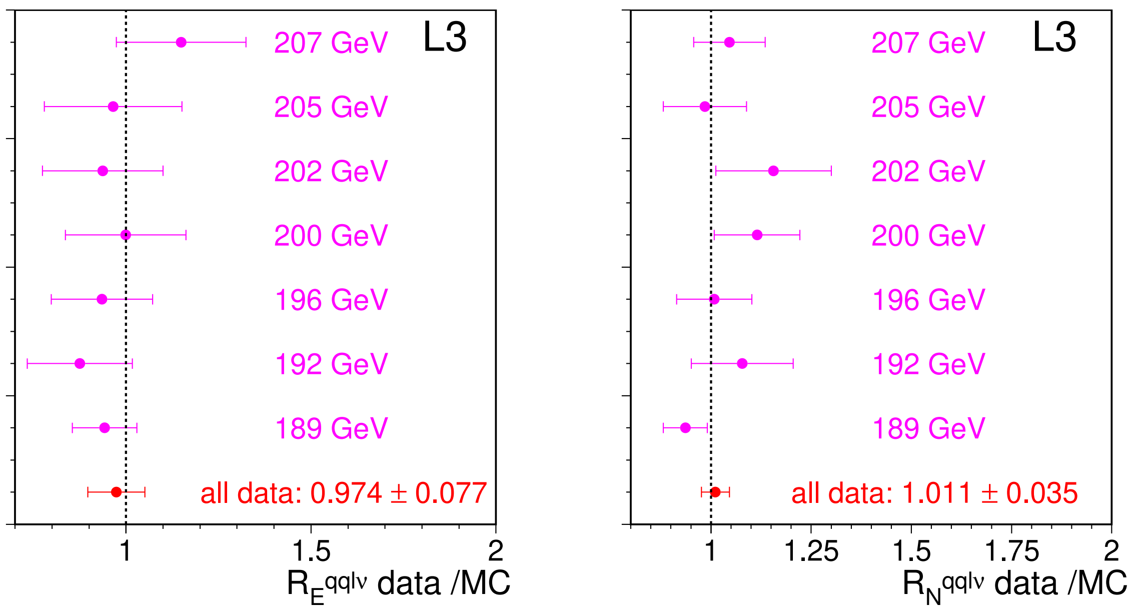

Figure 13: The ratio $R_E^{qql\nu}$ and $R_N^{qql\nu}$ at detector level for the various energy samples and for the complete data set.

4 Comparison with models

The R_E and R_N values predicted by PYTHIA NoCR, SKII and SKI CR models are given in Table 5 for 189$\leq \sqrt{s} \leq$ 207 GeV.

Model	R_N detector	R_E detector
No CR	0.918 ± 0.003	0.672 ± 0.003
SkII	0.916 ± 0.003	0.667 ± 0.003
SKI (k_I=0.6)	0.896 ± 0.003	0.659 ± 0.003
SKI (k_I=3.0)	0.843 ± 0.003	0.631 ± 0.003
SKI 100%	0.762 ± 0.003	0.581 ± 0.003

Table 5: Model predictions for R_E and R_N obtained for $\sqrt{s}$=189-207 GeV.

From these numbers we see that the data prefer weak colour reconnection effects when compared to PYTHIA model. R_E and R_N which may be sensitive to different systematic effects are giving consistent results. Figure 14 shows the comparison of R_N measured at 189$\leq \sqrt{s} \leq$ 207 GeV with the different Monte Carlo model predictions.

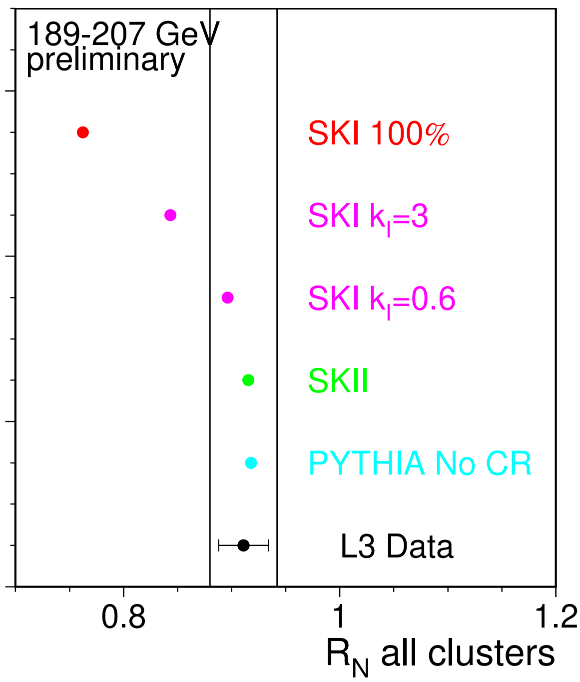

Figure 14: The ratio R_E and R_N at detector level for several Monte Carlo models with and without Colour Reconnection. The black dot with the error bar shows the data with the statistical error only while the band corresponds to the sum in quadrature of the statistical and systematic error components.

The dot with error shows the data value with the statistical error only while the band width corresponds to the total error taken as the sum in quadrature of the statistical and systematic components.

Since the sensitivity of R_E is smaller than for R_N and that the two variables are strongly correlated the following results are based only on R_N.

The dependence of R_N on the reconnection probability has been investigated with the SKI model. For this we have used four Monte Carlo samples: the one generated with 100% reconnection probability, the samples with k_I=0.6 and 3.0 and the No CR sample. In the SKI model the fraction of reconnected events is controlled by the k_I parameter and a parameterisation of the ratio dependence on k_I has been attempted with the four MC samples produced at different k_I. Figure 15 (top) shows the k_I dependence of R_N measured from MC (open circles). The line is a fit of a function of the form $R_N(k_I) = p_1(1 - exp(-p_2 k_I)) + p_3$ to the R_N MC values given in Table 5. The black point is the L3 measurement with the horizontal band showing

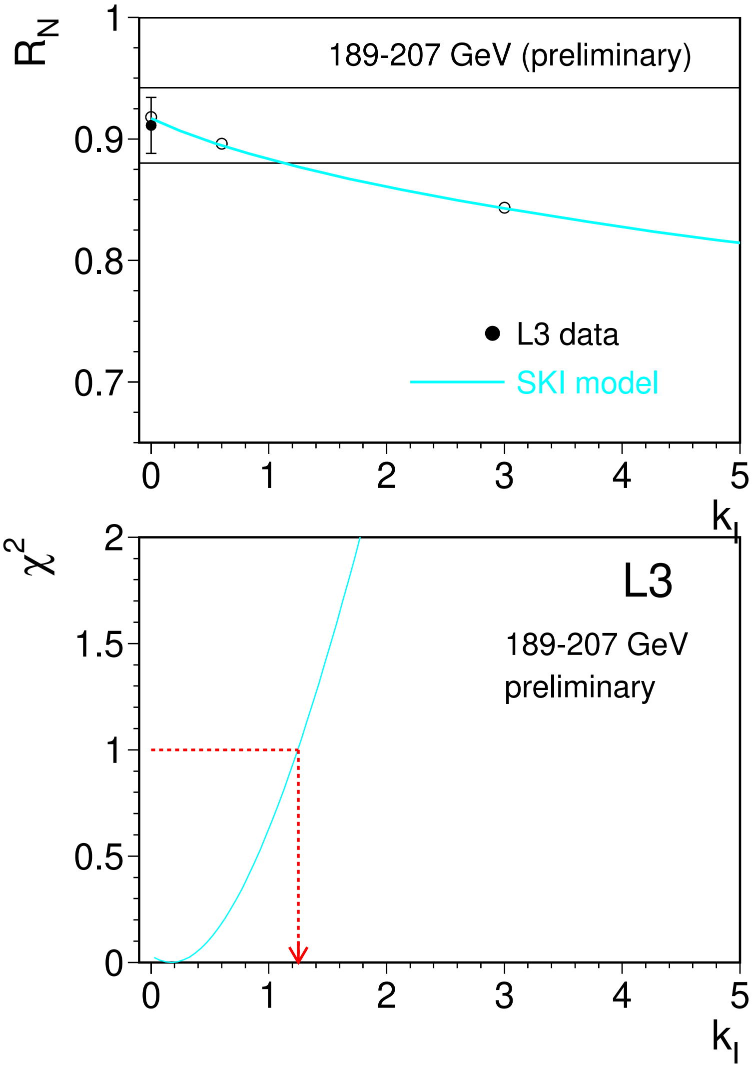

Figure 15: a) The ratio R_N fitted as a function of k_I for the SKI model(open circle). The black dot with the error bar shows the data with the statistical error only while the band corresponds to the sum in quadrature of the statistical and systematic error components. b) $\chi 2$ distribution as a function of k_I obtained by comparing the data to the SKI predicted dependence.

the 1 sigma boundary including the systematic error. A χ^2 between data and Monte Carlo is evaluated as a function of k_I and the result is shown in figure 15 (bottom). This curve gives a minimum at k_I=0.17, corresponding to about 11% reconnection probability if computed at $\sqrt{s}$=189 GeV, with a large uncertainty making the result also consistent with no CR effect. Then an upper limit $k_I < 1.25$ is obtained at 68% CL using the whole L3 data sample. This value should correspond to a reconnection probability of about 46% at $\sqrt{s}$ = 189 GeV which can be also translated into a W mass shift less than 40 MeV at $\sqrt{s}$=189 GeV.

In this study the comparison with ARIADNE and HERWIG models is done with the special Monte Carlo samples generated with the ALEPH parameters and fully simulated in the L3 detector [1)]. In order to use these large samples produced only at $\sqrt{s}$=189 GeV it is necessary to correct the values measured at each centre-of-mass energy to a value at the common centre-of-mass energy of 189 GeV.

5 Results scaled to $\sqrt{s}$= 189 GeV

The correction which is applied to a value of R_N measured at a particular $\sqrt{s}$ is obtained from a parametrisation of the R_N energy dependence as obtained using Monte Carlo models. This parametrisation corresponds to a fit of a second order polynomial function to the predicted dependence shown in Figure 10. The fit has been performed with PYTHIA No CR model and with various SKI model predictions (k_I= 3 and the SK1(100%)) to estimate the systematic uncertainty coming from the model choice. Figure 16 shows the result of the 3 different fits. The 3 models give similar results. The parametrisation used as default is the one obtained with PYTHIA NoCR giving: $R_N(\sqrt{s})/R_N^{189GeV} = -3.0710^{-3}s + 0.1297\sqrt{s} - 12.56$.

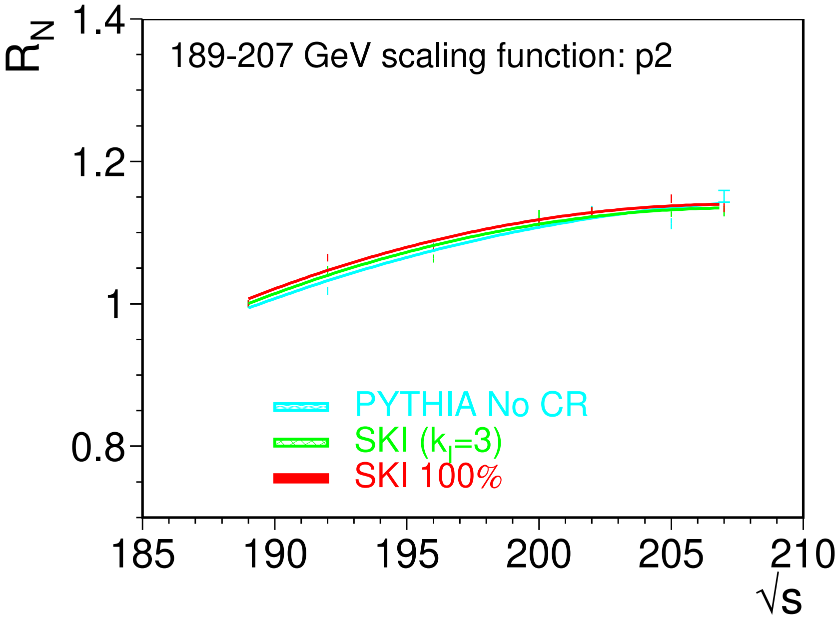

Figure 16: Results of fitting the ratio R_N predicted by various PYTHIA schemes as a function of $\sqrt{s}$ with a second order polynomial function.

Figure 17 shows the R_N values measured at all energies after rescaling to 189 GeV using the previous function. Since the systematic errors are fully correlated among the different energies a weighted average using the statistical error only is performed. The R_N^{189GeV} value obtained with the complete data set is then:

$$R_N^{189GeV} = 0.844 \pm 0.022(stat.) \pm 0.021(syst.) \pm 0.002(rescale)$$

[1)]These Monte Carlo samples (called Cetraro files) are part of a set produced for common systematic studies among the 4 LEP collaborations

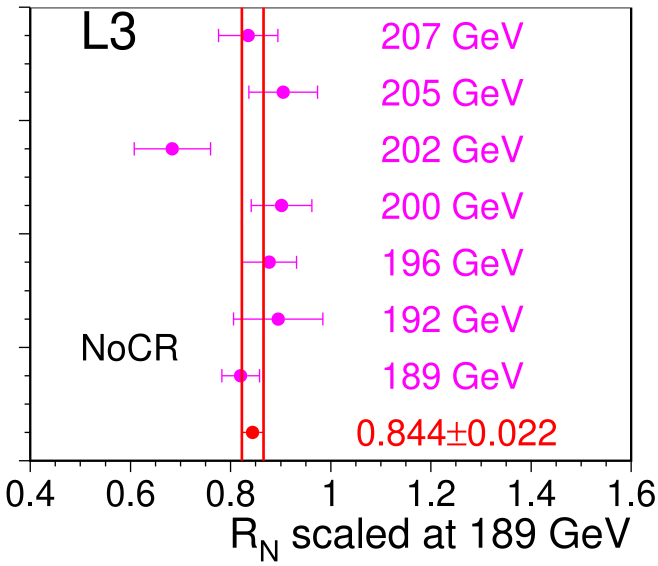

Figure 17: The R_N values rescaled to 189 GeV together with the average value. The errors shown are statistical only.

The third uncertainty quoted correponds to an additional systematic uncertainty coming from the model dependence of the parametrised function. It is estimated by doing the difference of the average obtained with the No CR model and the average obtained with the SKI CR model with k_I=3 This uncertainty is rather small.

6 Comparison with the common Monte Carlo files

The previous result can be compared with the common LEP Monte Carlo samples of KORALW events produced at $\sqrt{s}$=189 GeV. The available samples correspond to different fragmentation schemes applied to the same generated partons. The JETSET, ARIADNE and HERWIG with and without CR have been used. The R_N values obtained with these models are summarised in Tables 6 and 7. A statistics of 250 K has been used for each model. The values obtained with the L3 PYTHIA Monte Carlo samples generated at 189 GeV are also given in Table 6 for comparisons.

The JETSET and SKI predictions from the common files show a similar behaviour as the one seen with the L3 PYTHIA Monte Carlo samples. However the difference between the full reconnection and the No-CR scenario is less for the common files. [2)]

In the case of ARIADNE and HERWIG common samples, the CR schemes implemented in these two models are not modifying significantly the particle flow distributions. All the distributions built from particle between jets are consistent with the distributions without CR. This is illustrated in Figure 18 showing the ratio distributions as a function of the rescaled angle for these two models with and without CR. A study has also been done with the asymmetry variables introduced in Reference [5] to complement the particle flow analysis. Both ARIADNE No CR and AR2 models agree within each other and with the data. The same conclusion has

[2)]This difference is due to the larger number of Monte Carlo sampling points used in the LEP samples to calculate the overlap integral (1000 instead of 100).

Model	P_{reco} (%)	R_N Common MC	R_N L3 MC
No CR	0.0	0.8622 ± 0.0037	0.8594 ± 0.0053
SKI(k_i=0.10)	7.2	0.8613 ± 0.0037	
SKI(k_i=0.15)	10.2	0.8598 ± 0.0037	
SKI(k_i=0.20)	13.4	0.8585 ± 0.0037	
SKI(k_i=0.25)	16.1	0.8561 ± 0.0037	
SKI(k_i=0.35)	21.4	0.8551 ± 0.0037	
SKI(k_i=0.45)	25.9	0.8509 ± 0.0036	
SKI(k_i=0.60)	32.1	0.8482 ± 0.0036	0.8515 ± 0.0053
SKI(k_i=0.80)	39.1	0.8414 ± 0.0037	
SKI(k_i=1.00)	44.9	0.8381 ± 0.0036	
SKI(k_i=1.50)	55.9	0.8318 ± 0.0036	
SKI(k_i=3.00)	72.8	0.8135 ± 0.0036	0.7879 ± 0.0052
SKI(k_i=5.00)	82.5	0.7989 ± 0.0035	
SKI(100%)	100.0	0.7482 ± 0.0033	0.7090 ± 0.0048

Table 6: JETSET NoCR and SKI Model predictions for R_N obtained with the common LEP samples at $\sqrt{s}$=189 GeV. The second column gives the fraction of reconnected events in the common samples obtained for the different choice of k_I values. The numbers given in the last column correspond to PYTHIA predictions obtained from the L3 Monte Carlo samples.

Model	R_N Common MC
ARIADNE No CR	0.8754 ± 0.0037
ARIADNE AR2	0.8696 ± 0.0037
HERWIG No CR	0.8822 ± 0.0038
HERWIG CR	0.8805 ± 0.0037

Table 7: ARIADNE and HERWIG Model predictions for R_N obtained with the common LEP samples at $\sqrt{s}$=189 GeV

been reached with HERWIG NoCR and HERWIG CR. According to these observations, one should not expect with these models significant effect on the reconstructed W mass from 4 jet events. This point is under investigation.

7 Conclusions

The study of the particle flow distributions in hadronic W pair decays to search for colour reconnection effects have been performed on the L3 data collected at $\sqrt{s}$ =189 GeV up to 208 GeV. From this search, no strong colour reconnection effect is observed using the LEP2 data.

The results obtained with the data have been compared to the SKI CR model implemented in PYTHIA. The data are consistent with small reconnection probability. In the SKI framework the preferred value corresponds to about 11% of reconnection probability. Taking into account the uncertainty the result is translated into a 68% CL limit on the parameter $k_I < 1.25$.
A comparison with ARIADNE and HERWIG have shown that the CR schemes implemented in these two models are not modifying the interjet particle activity in the hadronic W pair decay

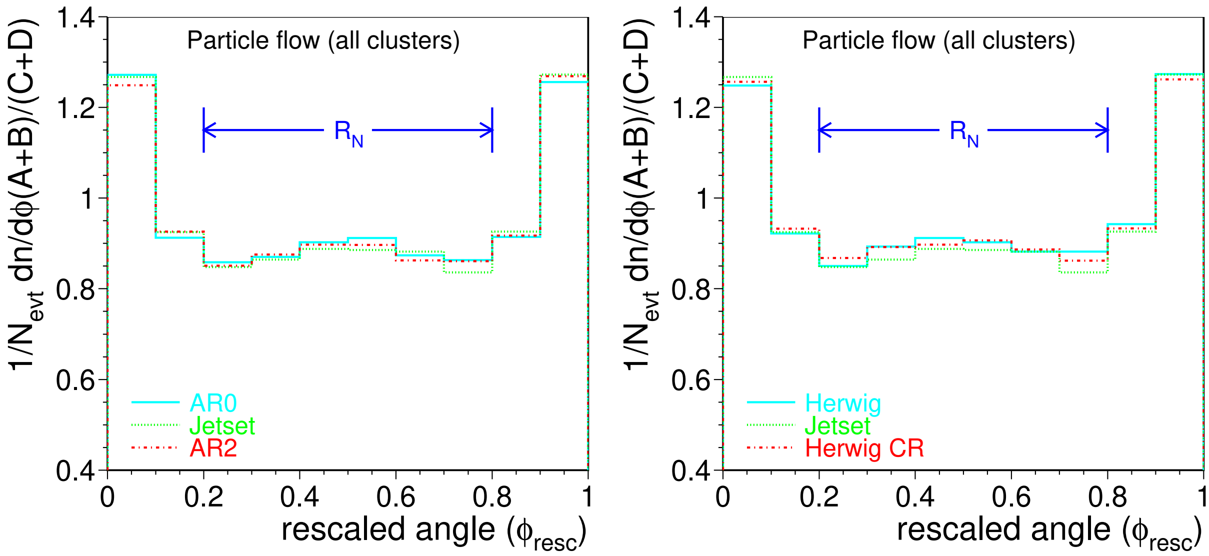

Figure 18: Ratio (R) of the flow distribution in regions (A+B) divided by the flow distribution in regions (C+D) for ARIADNE on the left and for HERWIG on the right. The JETSET NoCR prediction is also given for comparison.

events, thus limiting the possibility to constrain or rule out any of these models.

References

[1] G. Gustafson, U. Pettersson and P. Zerwas, Phys. Lett. **B 209** (1988) 90.

[2] T. Sjöstrand and V. Khoze, Z. Phys. **C 62** (1994) 281; V. Khoze and T. Sjöstrand, Eur. Phys. J. **C 6** (1999) 271.

[3] G. Gustafson and J. Häkkinen, Z. Phys. **C 64** (1994) 659.

[4] Proceedings of the workshop "Physics at LEP 2", CERN Yellow Report 96-01.

[5] D. Duchesneau, "*New method based on energy- and particle-flow in* $e^+e^- \rightarrow W^+W^- \rightarrow$*hadrons events for colour reconnection studies*", preprint LAPP-EXP 2000-02; "*Studies of Colour Reconnection Effects in Hadronic W pair Decays at LEP*", Nucl. Phys. B (Proc. Suppl.) **96** (2001) 13.

[6] L3 Collab, B. Adeva et al., Nucl. Instr. and Meth. **A 289** (1990) 35;
M. Chemarin et al., Nucl. Instr. and Meth. **A 349** (1994) 345;
M. Acciarri et al., Nucl. Instr. and Meth. **A 351** (1994) 300;
G. Basti et al., Nucl. Instr. and Meth. **A 374** (1996) 293;
I. C. Brock et al., Nucl. Instr. and Meth. **A 381** (1996) 236;
A. Adam et al., Nucl. Instr. and Meth. **A 383** (1996) 342.

[7] The L3 Collaboration, *Search for Colour Reconnection Effects in* $e^+e^- \rightarrow W^+W^- \rightarrow$ *hadrons*, L3 Note 2560 (2001), submitted to the 2001 Winter Conferences.

[8] KK2F Monte Carlo Program:
S. Jadach, B. F. L. Ward and Z. Wąs, Phys. Lett. **B449** (1999) 97.

[9] PYTHIA Monte Carlo Program:
T. Sjöstrand, CERN-TH-7112/93 (1993), revised august 1995;
T. Sjöstrand, Comp. Phys. Comm. **82** (1994) 74.

[10] ARIADNE Monte Carlo Program:
L. Lönnblad, Comp. Phys. Comm. **71** (1992) 15.

[11] HERWIG Monte Carlo Program:
G. Corcella et al.,JHEP **0101** (2001) 010 [hep-ph/0011363]; hep-ph/0201201;
G. Marchesini et al., Comp. Phys. Commun. **67** (1992) 465.

[12] L. Lönnblad, Z. Phys. C **70** (1996) 107.

[13] B. Webber, J. Phys. G **24** (1998) 2.

[14] A. Ballestrero et al., *Report of the QCD Working Group*, preprint hep-ph/0006259 (2000).